

---

## Foul-weather friends: Modelling thermal stress mitigation by symbiotic endolithic microbes in a changing environment

Zardi Gerardo I. <sup>1</sup>, Monsinjon Jonathan <sup>1</sup>, McQuaid Christopher D. <sup>1</sup>, Seuront Laurent <sup>1,2,3</sup>, Orostica Mauricio <sup>1</sup>, Want Andrew <sup>4</sup>, Firth Louise B. <sup>5</sup>, Nicastro Katy R. <sup>1,6,\*</sup>

<sup>1</sup> Rhodes Univ, Dept Zool & Entomol, ZA-6140 Grahamstown, South Africa.

<sup>2</sup> Univ Littoral Cote d'Opale, Univ Lille, CNRS, UMR 8187, LOG, Lab Oceanol & Geosci, Lille, France.

<sup>3</sup> Tokyo Univ Marine Sci & Technol, Dept Marine Energy & Resources, Minato Ku, Tokyo, Japan.

<sup>4</sup> Heriot Watt Univ, Int Ctr Isl Technol, Orkney Campus, Stromness, Scotland.

<sup>5</sup> Univ Plymouth, Sch Biol & Marine Sci, Plymouth, Devon, England.

<sup>6</sup> Univ Algarve, CIMAR Associated Lab, CCMAR, Faro, Portugal.

\* Corresponding author : Katy R. Nicastro, email address : [katynicastro@gmail.com](mailto:katynicastro@gmail.com)

---

### Abstract :

Temperature extremes are predicted to intensify with climate change. These extremes are rapidly emerging as a powerful driver of species distributional changes with the capacity to disrupt the functioning and provision of services of entire ecosystems, particularly when they challenge ecosystem engineers. The subsequent search for a robust framework to forecast the consequences of these changes mostly ignores within-species variation in thermal sensitivity. Such variation can be intrinsic, but can also reflect species interactions. Intertidal mussels are important ecosystem engineers that host symbiotic endoliths in their shells. These endoliths unexpectedly act as conditionally beneficial parasites that enhance the host's resistance to intense heat stress. To understand how this relationship may be altered under environmental change, we examined the conditions under which it becomes advantageous by reducing body temperature. We deployed biomimetic sensors (robomussels), built using shells of mussels (*Mytilus galloprovincialis*) that were or were not infested by endoliths, at nine European locations spanning a temperature gradient across 22 degrees of latitude (Orkney, Scotland to the Algarve, Portugal). Daily wind speed and solar radiation explained the maximum variation in the difference in temperature between infested and non-infested robomussels; the largest difference occurred under low wind speed and high solar radiation. From the robomussel data, we inferred body temperature differences between infested and non-infested mussels during known heatwaves that induced mass mortality of the mussel *Mytilus edulis* along the coast of the English Channel in summer 2018 to quantify the thermal advantage of endolith infestation during temperature extremes. Under these conditions, endoliths provided thermal buffering of between 1.7 degrees C and 4.8 degrees C. Our results strongly suggest that sustainability of intertidal mussel beds will increasingly depend on the thermal buffering provided by endoliths. More generally, this work shows that biomimetic models indicate that within-species thermal sensitivity to global warming can be modulated by species interactions, using an intertidal host-symbiont relationship as an example.

---

**Keywords** : biophysical model, climate change, mussels, mutualism, thermal tolerance

49

## 50 INTRODUCTION

51 Globally, extreme temperature events have risen in frequency, strength and duration  
52 (e.g., Oliver et al., 2018) and are predicted to become more severe with intensifying climate  
53 variability (Fischer et al., 2010; Rahmstorf et al., 2011). Recently, extended periods of  
54 anomalously high temperatures such as heatwaves have driven significant ecological changes  
55 (e.g., Hughes et al., 2017; Smale et al., 2019; Wernberg et al., 2013). Given the serious  
56 consequences for biodiversity and ecosystem functioning, there is increasing interest in  
57 understanding variability in within-species thermal tolerance; we have yet to understand why  
58 some individuals survive when conspecifics succumb to abrupt temperature increases. The  
59 appreciation of such within-species variability will aid the prediction of long-term responses by  
60 species as a whole. Identifying the full capacity of species to survive heatwaves and extreme  
61 heat stress events may offer crucial insights into the stability of their ecological, and socio-  
62 economic functions.

63 Intertidal ecosystems are among the most productive of ecosystems, supplying vital  
64 services such as food production, stabilization of shorelines, capture of 'blue carbon', water  
65 clearance, nutrient turnover and acting as nurseries for high-trophic level taxa (e.g., Costanza  
66 et al., 1997; Macreadie et al., 2019; Raffaelli et al., 2012). Due to their daily exposure to both  
67 aerial and marine conditions and their low thermal inertia compared to open-ocean waters,  
68 these ecosystems are particularly vulnerable to extreme climatic events such as heatwaves  
69 and coldwaves (Halpern et al., 2008). Heatwaves in particular, have drastic deleterious effects  
70 on intertidal ecosystems globally. Heatwave-induced mass mortalities, local extinctions and  
71 range contractions of numerous key benthic habitat-forming species (e.g., corals, seagrasses,  
72 macroalgae, bivalves) have resulted in depleted local biodiversity, reduced carbon  
73 sequestration and weakened natural coastal defences (Arias-Ortiz et al., 2018; Holbrook et  
74 al., 2020). The damage caused by heatwaves also reduces the socioeconomic value of these

75 ecosystems by reducing recreational activities and tourism (e.g., Smale et al., 2019; Stillman,  
76 2019) with major direct economic damage to recreational, artisanal and commercial fisheries  
77 (e.g., FAO, 2020; Li et al., 2019).

78         Mussel die-offs induced by heatwaves exemplify the severe economic and ecological  
79 effects of extreme heat events. Intertidal mussels are dominant ecosystem engineers that  
80 provide crucial habitat, supporting biodiversity and underpinning myriad ecosystem functions  
81 and services. For example, evidence from the NE Pacific coast and from southern African  
82 rocky shores shows that hundreds of associated species (e.g. invertebrates, small fish and  
83 algae) depend on mussel aggregations (Nicastro et al., 2020; Suchanek, 1985). Their dense  
84 mono- and multi-layered beds remain moist and thermally benign during low tides and offer  
85 protection against wave action during high tide (Helmuth et al., 2016). The loss of mussel beds  
86 associated with recent warming trends has resulted in the decline of species richness and the  
87 alteration of community structure (Harley, 2011).

88         Numerous experimental and observational studies have shown that symbiotic  
89 interactions, both parasitic and mutualistic, have dramatic effects on the host organism  
90 (Chomicki et al., 2020; Firth et al., 2017). Such interactions can alter the host's experience of  
91 environmental stress by altering the host phenotype (Feldhaar, 2011), with consequences for  
92 host fitness (i.e., survival and fecundity). When the host species is an ecosystem engineer,  
93 such as a mussel, these interactions can have significant knock-on effects at population,  
94 community and ecosystem levels (Fellous et al., 2009). As thermal stress intensifies under  
95 climate change, the effect of symbionts on the temperature tolerance of their hosts will be  
96 particularly important. Parasites can drive considerable alterations to both their host's thermal  
97 performance optima (Gehman et al., 2018) and thermal preferences (Macnab et al., 2012). In  
98 turn, mutualisms can favour survival following exposure to heat stress (Brumin et al., 2011;  
99 Feldhaar, 2011). Because gradual warming and the increased stress of extreme heat events

100 will challenge individuals with and without symbionts, mutualistic relationships will have a  
101 major role in setting within-species thermal variability (Feldhaar, 2011).

102 Critically, the nature of symbiotic associations is context dependent; a single symbiotic species  
103 can have both positive and negative effects depending on the biotic/abiotic environment in  
104 which the interaction occurs (e.g., Altizer et al., 2013; Harvell et al., 2009; Nowakowski et al.,  
105 2016; Sauer et al., 2018). The gradual change between symbiotic states may confer a suite  
106 of novel traits to the host organism thus offering it ecological opportunities (*sensu* Janson et  
107 al., 2008) that would otherwise be unavailable. This is the case for the widespread symbiosis  
108 between shell-degrading endolithic cyanobacteria and intertidal mussels (Zardi et al., 2016).  
109 Until recently, numerous studies have described a multitude of negative (lethal and sub-lethal)  
110 effects of endolith corrosion in mussels (Marquet et al., 2013), stressing the  
111 parasitic nature of this relationship (Zardi et al., 2009). Endoliths are metabolically dependent  
112 on the host for CO<sub>2</sub> released during shell degradation, which they use for photosynthesis  
113 (Garcia-Pichel et al., 2010). As a result, endoliths can affect the host's energetic budgeting  
114 through their boring activity at the expense of byssal attachment strength, growth and  
115 reproduction (Kaehler et al., 1999; Marquet et al., 2013; Ndhlovu et al., 2021; Nicasro et al.,  
116 2018; Zardi et al., 2009). Importantly, recent results have shown that shell corrosion caused  
117 by endoliths mitigates the thermal stress experienced by their mussel hosts; mussels with  
118 corroded shells experience significantly lower body temperatures leading to significant  
119 increases in survival (up to 50%) during heatwaves compared to conspecifics that are not  
120 affected by endoliths (Zardi et al., 2016). Such conditional help (*sensu* Fellous & Salvaudon,  
121 2009) is triggered by reduced absorption of solar energy by mussel shells that are whitened  
122 by endolithic boring (Gehman et al., 2019; Zardi et al., 2016).

123 Despite a growing number of studies reporting the incidence and effects of  
124 phototrophic shell-degrading endoliths in a variety of taxa and habitats, the key environmental  
125 factors that determine the nature of the relationship remain unknown. This study aims at  
126 understanding the limits of endolith-mediated protection against thermal stress across

127 environments. Such knowledge is pivotal to the development of realistic, large-scale  
128 predictions of how mussel beds will respond to environmental change and the consequences  
129 to their related ecosystem and socio-economic value. To achieve this, we built biomimetic  
130 temperature loggers using the shells of *Mytilus galloprovincialis* that were either heavily  
131 infested or not infested by endoliths. These were then deployed in the field across a wide  
132 latitudinal range (i.e., 37°N to 59°N) to assess changes in endolithic thermal buffering in a  
133 variable environment and to identify the drivers of the maximum temperature differences  
134 between non-infested and infested mussels. Data from the biomimetic temperature loggers  
135 and high-resolution weather data were then used in Generalized Linear Mixed Models to  
136 identify the environmental factors influencing the cooling effect of endoliths on mussel  
137 populations. We subsequently used the model to identify maximum body temperature  
138 differences between infested and non-infested mussels under the known conditions of a heat  
139 wave-induced mortality event of *Mytilus edulis* that occurred along the north French coast in  
140 summer 2018. In parallel, we assessed whether non-infested mussels warm up faster than  
141 infested individuals as expected for dark ectotherms vs paler ones (Moyen et al., 2019; Porter  
142 et al., 1969).

143

## 144 **METHODS**

### 145 **Drivers of the maximum temperature difference between non-infested and infested** 146 **mussels**

147 Biomimetic temperature loggers (robomussels) are used to mimic the thermal characteristics  
148 of living mussels (Helmuth et al., 2010; Helmuth et al., 2016). In this study, robomussels were  
149 deployed at multiple locations across a wide latitudinal range and environmental gradient  
150 along North Atlantic shores to quantify differences in body temperatures of mussels with and  
151 without endoliths when exposed to natural variability in meteorological conditions. All  
152 robomussels were assembled using the emptied shells of *Mytilus galloprovincialis* (shell length

153 4-5 cm) sampled at Viana do Castelo (Portugal; 41°42'0.94"N, 8°51'25.59"W) from wave  
154 exposed intertidal rocky shores composed of granite. Mussels were sampled within a  
155 monolayered bed (i.e. all individuals attached directly to the substratum) in a sun-exposed  
156 area (i.e. surfaces with limited shading, exposed to solar radiation 60 % of the day). Shells  
157 were either non-infested (Group A; Zardi et al., 2009) or heavily infested by endoliths (Group  
158 D; Fig. 1a); Group A shells have clean, intact periostracum and distinct periostracal striation,  
159 Group D shells are severely pitted and deformed, and the outer striations on the periostracum  
160 are almost completely absent. Robomussels were made by placing a temperature logger  
161 (iButtons®, DS1922, Maxim Integrated Products, Dallas Semiconductor, USA, resolution =  
162 0.5 °C, accuracy = 0.5 °C) between two empty mussel valves filled with silicone sealant and  
163 leaving it to dry at air temperature for 48 hours before being deployed in trials (Nicastro et al.,  
164 2012). Endoliths in infested shells were killed by keeping the mussel shells in boiling water for  
165 an hour before assembling them (Zardi et al., 2016). Loggers recorded temperatures at 30-  
166 min intervals from 1<sup>st</sup> August to 13<sup>th</sup> September 2017, for a period of 42 days at nine sites (Fig.  
167 1b; Supplementary Table S1). Data were lost from Plymouth (UK) due to robomussels being  
168 vandalised. For one site (Aberffraw, UK), deployment was done the following summer, from  
169 28<sup>th</sup> July to 18<sup>th</sup> September 2018. At each site, three to six pairs of infested and non-infested  
170 robomussels were glued to the substratum (Z-spar Splash zone, A-788) in the mid mussel  
171 zone on a relatively flat slope, orientated like a living solitary mussel (i.e., longitudinal axis  
172 oriented parallel to the substratum with the ventral side facing the substratum) and equidistant  
173 from each other (approximately 10 cm).

174 At each site, average estimates of robomussel intertidal height were calculated using the  
175 temperature logger profiles and tables of tidal heights (Gilman et al., 2006; Harley et al., 2003).  
176 These profiles clearly reveal when robomussels are first inundated by the returning tide  
177 through a sudden sharp drop in temperature. The time of tidal inundation was used to calculate  
178 the Effective Shore Level (ESL) using the XTide software (<https://flaterco.com/xtide/>). Tidal  
179 predictions were obtained for nearby maritime ports (Supplementary Table S2). For every

180 robomussel pair, we retrieved all tidal levels that were associated with a temperature drop of  
181  $>8^{\circ}\text{C}$  in 30 min during incoming tides. We chose this threshold, which corresponds to a  $5.33^{\circ}\text{C}$   
182 drop in 20 min, to ensure reliability of ESL estimates while maximising the probability of finding  
183 at least one drop during the study period (Gilman et al., 2006). We calculated the mean ESL  
184 ( $\pm$  standard deviation; SD) for each robomussel pair (Supplementary Table S3). ESLs were  
185 used to determine when mussels were exposed/submerged. However, ESLs can vary daily  
186 due to surge and wave exposure, which might lead to the misidentification of  
187 exposed/submerged periods. To ensure that temperature data were correctly attributed to  
188 periods of submergence or aerial exposure, we kept data that were recorded above the upper  
189 limit of a buffer zone (mean ESL + 0.3 m) or below the lower limit of a buffer zone (mean ESL  
190 - 0.3 m). Temperature data during submergence were used as a control, as we expect no  
191 differences in temperature between non-infested and infested robomussels when submerged.  
192 We used Linear Mixed Effects models (LMEs; using 'nlme' R package; Pinheiro et al., 2020)  
193 to test this. After adding robomussel identity as a random effect and controlling for  
194 autocorrelation (autoregressive model of order 1), we found that non-infested mussels were,  
195 on average, significantly warmer than infested ones during aerial exposure (mean difference  
196 =  $0.36^{\circ}\text{C}$ , SD = 2.04,  $t = -2.14029$ ,  $p = 0.0323$ ) whereas we did not find a significant difference  
197 during submergence ( $t = -1.62900$ ,  $p = 0.1033$ ). Therefore, we kept only temperature data  
198 during emergence for further analysis.

199 Using robomussels as proxy for mussel body temperature (Helmuth et al., 2010;  
200 Helmuth et al., 2016), we expected the maximum difference between non-infested and  
201 infested mussels (calculated as non-infested minus infested temperatures for each  
202 robomussel pair) to vary geographically during emergence due to site-specific meteorological  
203 conditions. Meteorological variables that are considered determinants of the body temperature  
204 of invertebrates (i.e. air temperature, wind speed, precipitation, relative humidity, and solar  
205 radiation (Helmuth, 1998)) were obtained from nearby weather stations (Supplementary Table



206 S4). However, we excluded three of our nine study sites from this analysis because solar  
207 radiation was not measured at these sites during the study period (Supplementary Table S4).  
208 Weather station data in the United Kingdom (Met Office, 2019a, 2019b, 2019c), France and  
209 Portugal were provided by the Centre for Environmental Data Analysis (CEDA;  
210 <http://data.ceda.ac.uk/badc/ukmo-midas-open/data/>), Météo-France  
211 (<https://donneespubliques.meteofrance.fr/>) and Instituto Português do Mar e da Atmosfera  
212 (IPMA; <https://www.ipma.pt/en/otempo/obs.superficie/>), respectively.

213 We used Generalized Linear Mixed Models (GLMMs; using 'lme4' R package; Bates et  
214 al., 2015) to test for effects of daily values of (i) mean air temperature ( $^{\circ}\text{C}$ ), (ii) mean wind  
215 speed ( $\text{m s}^{-1}$ ), (iii) total precipitation (mm), (iv) mean relative humidity (%), and (v) total (global)  
216 solar radiation ( $\text{J m}^{-2}$ ) on the daily maximum difference in temperature between non-infested  
217 and infested robomussels during emergence. Meteorological variables were averaged (or  
218 summed for solar radiation and precipitation) within robomussel pair-specific periods of  
219 emergence. The identity of individual pairs of robomussels was included as a random factor  
220 nested within study site to account for inter- and intra-site variance. Because our dependant  
221 variable was non-normally distributed (positively skewed), we used GLMMs with a Gamma  
222 distribution and excluded the few days during which non-positive temperature differences  
223 were found between paired robomussels. We applied a log link function to stabilize the  
224 variance of residuals. We fitted all models (i.e. all combinations of response variables) using  
225 maximum likelihood and selected the best candidates based on the lowest value of Akaike  
226 Information Criteria corrected for finite sample size (AICc) and Akaike weights, which give a  
227 measure of the relative support for each model (Akaike, 1974; Burnham et al., 2002). We  
228 considered models with  $\Delta\text{AICc} < 2$  as competitive and, for the sake of parsimony, we retained  
229 the model with the least number of parameters. Based on this model, we extrapolated daily  
230 maximum differences in body temperature between non-infested and infested mussels under  
231 a range of meteorological conditions likely to be encountered on the shore.

232 **Quantifying the thermal advantage of infestation during a heatwave-induced mussel**  
233 **mortality event**

234 To assess the extent of thermal buffering provided by endoliths during extreme hot weather  
235 conditions, we used the meteorological data at Wimereux, France, during summer 2018 where  
236 mass mortality events of *Mytilus edulis* occurred following heatwaves (Seuront et al., 2019).  
237 Nine heatwaves (ranging from moderate to severe; see Table 2) were identified based on air  
238 temperature, following Hobday et al. (2018). We extracted meteorological data during these  
239 periods and predicted the daily maximum temperature difference between non-infested and  
240 infested mussels based on the previously selected model.

241 **Assessing heating rate and maximum body temperature during aerial exposure**

242 Temperatures recorded by robomussels were used as proxy of the body temperatures of living  
243 mussels. To assess whether non-infested mussels warm up faster and reach higher body  
244 temperatures than infested ones during aerial exposure, we calculated the rate of change in  
245 body temperature as well as the maximum and near-maximum (95<sup>th</sup> percentile) body  
246 temperature for each robomussel during aerial exposure for every tidal cycle. We calculated  
247 the average rate of change in body temperature during one tidal cycle using the slope of the  
248 linear regression between temperature and time data (converted to °C h<sup>-1</sup>). A positive slope  
249 indicates that robomussels were warming up while a negative one indicates that robomussels  
250 were cooling down. We assessed potential differences between non-infested mussels and  
251 infested ones using Linear Mixed Effects models with robomussel identity included as a  
252 random effect.

253

254 **RESULTS**

255 **The thermal buffering effect of infestation depends on solar radiation and wind speed**

256 Five candidate models were retained, with the number of selected meteorological parameters  
257 varying from two to four (Table 1). When compared to the null model (i.e., assuming no effect  
258 of any meteorological parameters; Table 1), these models exhibit a better fit (Table 1). The  
259 two best models (i.e., those with the lowest AICc values) showed similar relative support  
260 (Akaike weights > 0.2; Table 1) and, for the sake of parsimony, we selected the simplest one  
261 (i.e., using solar radiation and wind speed; Table 1) for further analysis. The results suggest  
262 that solar radiation ( $t = 8.609$ ,  $p < 0.0001$ ) and wind speed ( $t = -3.181$ ,  $p = 0.00147$ ) are the  
263 main drivers of the maximum difference in body temperature between non-infested and  
264 infested mussels. The selected model appropriately reproduced measured temperature  
265 differences, albeit slightly underestimating the difference at high temperatures  
266 (Supplementary Fig. S1). On average, daily total solar radiation during emergence increased  
267 from northern to southern sites with greater variability measured at the three northernmost  
268 (NEB, SKA and ABE) and intermediate (WIM) sites considered (Fig. 1c). Daily mean wind  
269 speed showed the opposite trend; decreasing to the south and again with greater variability  
270 measured at the three northernmost sites. Note that the southernmost site (VIL) was more  
271 exposed to wind than the other southern site (MON) during the study period. Geographically,  
272 the cooling effect of microbial endoliths (expressed as the maximum difference in body  
273 temperature between non-infested and infested robomussels predicted from the selected  
274 model using solar radiation and wind speed averaged over the study period) showed a  
275 gradient decreasing from southern (VIL and MON) to intermediate (WIM) and northern (NEB,  
276 SKA and ABE) sites (Fig. 1d). However, there was no clear pattern with latitude among the  
277 closest sites (e.g., MON and VIL). Confidence intervals of predictions (Fig. 1d) are shown in  
278 Supplementary Fig. S2 and the relationship between measured temperature differences and  
279 weather data is shown in Supplementary Fig. S3.

280

281 **Prediction of body temperature differences between non-infested and infested mussels**  
282 **during heatwaves**

283 In summer 2018 at Wimereux, based on the model that uses solar radiation and wind speed  
284 (see Table 1 and prediction surface in Fig. 1d), we predicted a cooling effect of microbial  
285 endoliths (i.e., the temperature difference between non-infested and infested mussels) of 4.21  
286 to 4.77°C during June heatwaves (which were classified as moderate to strong), of 2.75 to  
287 4.14°C during July heatwaves (which were classified as moderate to severe), and of 1.67 to  
288 3.97°C during August heatwaves (which were classified as moderate to strong; estimates are  
289 plotted on the prediction surface in Fig. 1d and confidence intervals are provided in Table 2).  
290 During most of these heatwaves, mussels were exposed to high solar radiation (noticeably  
291 higher than the conditions observed on average in southern sites like MON and VIL) and  
292 moderate wind speeds (similar to the conditions observed on average at all sites except ABE  
293 and MON; Fig. 1d). For one heatwave (10<sup>th</sup> August) that occurred under moderate solar  
294 radiation and high wind speed, the predicted temperature difference was rather low and similar  
295 to the ones predicted for northern sites (NEB, SKA and ABE).

296

### 297 **Non-infested mussels warm up faster and reach higher body temperatures than** 298 **infested mussels**

299 During periods of aerial exposure, non-infested robomussels warmed up faster than infested  
300 ones ( $t = -1.982$ ,  $p = 0.0475$ ; mean rate of change = 0.38 and 0.28 °C h<sup>-1</sup>, SD = 1.75 and 1.45,  
301 respectively; Fig. 2a). Non-infested robomussels also reached higher maximum temperatures  
302 than infested ones ( $t = -4.477$ ,  $p < 0.0001$ ; mean maximum temperature = 22.93 and 22.07°C,  
303 SD = 7.5 and 6.6, respectively; Fig. 2b). We obtained similar results when comparing near-  
304 maximum (95<sup>th</sup> percentile) temperatures ( $t = -4.098363$ ,  $p < 0.0001$ ; mean near-maximum  
305 temperature = 22.47 and 21.69°C, SD = 7.31 and 6.45, respectively for non-infested and  
306 infested ones; Fig. 2c).

307

## 308 **DISCUSSION**

309 We observed striking reductions in temperature in endolithically corroded robomussels  
310 compared to uncorroded ones in intertidal habitats, across large geographical areas exposed  
311 to a wide range of oceanographic and climatic conditions. Given that the biomimics used in  
312 this study have been extensively shown to be an accurate tool for recording organismal body  
313 temperature in their natural environment (e.g., Fitzhenry et al., 2004; Helmuth et al., 2016;  
314 Seabra et al., 2015), our results can effectively be interpreted as a marked cooling effect in  
315 infested mussels compared to non-infested mussels. Intraspecific variability in body  
316 temperature has to be accounted for in order to interpret and predict responses of the species  
317 to climatic change across biogeographic ranges. This is relevant not only for the individuals  
318 themselves, but also for the ecosystem as it provides crucial insights into the future stability of  
319 mussel beds and their role as ecosystem engineers that support myriad species, and a range  
320 of ecosystem functions and services.

321 We identify daily-mean wind speed and daily-total solar radiation as the environmental  
322 variables with the strongest influence on the within-site thermal buffering effects of endoliths.  
323 This is in agreement with previous work showing how body temperatures of intertidal  
324 ectothermic animals are primarily controlled by non-climatic heat sources, solar heating and  
325 re-radiation as opposed to climatic heat sources, i.e. air and water temperatures (e.g.,  
326 Helmuth, 2002; Marshall et al., 2010). Our results show a negative relationship between the  
327 two key variables, suggesting that the seasonality of wind and solar radiation most likely will  
328 shape the implications of our results. While the highest wind speeds typically occur during  
329 winter, the peak in solar radiation usually occurs in summer when thermal heat stress is at its  
330 highest. This means that the maximum endolithic thermal buffering occurs in summer when it  
331 is also most ecologically meaningful. In summer, during heatwave conditions recorded at  
332 Wimereux in France, body temperature differences between non-infested and infested  
333 mussels ranged between 1.7°C and 4.8°C. Like other intertidal organisms, mussels live close

334 to the upper limit of their physiological thermal tolerance window and such a remarkable level  
335 of thermal buffering due to phenotypic variation has the potential to trigger changes at the  
336 population level, particularly in areas where the survival and physiological performance of  
337 mussels have already been affected by increasing temperatures. Our findings show that  
338 uncorroded individuals have significantly higher maximum body temperature and faster  
339 heating rates than those of corroded mussels. In particular, heating rate is known to have  
340 significant effects on cardiac thermal performance in intertidal mussels; recent studies show  
341 that faster heating rates significantly increase the heart's critical temperature (i.e., the  
342 temperature triggering a precipitous decline of heart rate; Moyen et al., 2019). Critically, these  
343 studies also emphasise the complexity of abiotic and physiological interactions. Heating rates  
344 significantly affect the cardiac thermal tolerance, of high- but not low-zone mussels, while  
345 heavy mussels tend to heat up faster compared to light weight mussels- but at the fast-heating  
346 rate only.

347         The heating rates recorded in our study are lower than those previously reported in  
348 natural populations (e.g., Miller et al., 2017) or in laboratory experiments (e.g., Moyen et al.,  
349 2019 and references therein) and are thus unlikely to significantly affect heart rates, at least  
350 under our study conditions. Additionally, all mussels used to build robomussels were collected  
351 from the same site and mussel zone and had similar shell length, excluding any potential effect  
352 of body mass. Nevertheless, given the determinant role of intertidal height on mussel cardiac  
353 thermal tolerance, further investigation is needed to assess the effect of endolithic corrosion  
354 on heating rates and heart rates throughout the intertidal distribution of mussels and for  
355 different body masses. Framed in a more theoretical context, our results show that endoliths  
356 provide their host mussels with a *key innovation* (i.e., thermal buffering) that potentially offers  
357 an ecological opportunity, opening previously unexploited niches. Key innovations (termed "*ad*  
358 *hoc novelty*" in Feldhaar, 2011; Miller, 1949) are features that allow a species to interact with  
359 the environment in a different way and thus may provide the capacity, otherwise unavailable,

360 to exploit available resources (Galis, 2001; Hunter, 1998; Rabosky, 2014). For instance, in  
361 tropical dendrobatid poison frogs, the evolution of bright coloration as an advertisement of  
362 unprofitability to predators, reduces the function and thus the need for predator-induced  
363 “hiding” behaviour, thus offering novel habitat opportunities (Arbuckle et al., 2015; Santos et  
364 al., 2003; Summers, 2003). Another example is that of archer fish (*Toxotes* spp.) in which the  
365 evolved capacity to fire jets of water from their mouths to dislodge insects perched on  
366 overhanging foliage has opened access to new prey resources (Burnette et al., 2015;  
367 Schuster et al., 2006). Key innovations have been mainly investigated in an evolutionary  
368 context and are often described as a key and eventually an essential stimulus for adaptive  
369 radiation through “*the evolutionary divergence of members of a single phylogenetic lineage*  
370 *into a variety of different adaptive forms*” (Futuyma et al., 1988).

371         However, key innovations can be obtained through faster or even non-evolutionary  
372 routes. For instance, a variety of genome-engineering approaches have been used to reduce  
373 the proportion of black found on dairy cattle coats aiming at decreasing radiative heat gain, a  
374 contributing feature to heat stress (Maga, 2020). Similarly, alteration of a host’s life history  
375 traits triggered by symbionts may become advantageous under certain environmental  
376 conditions; fast-tracking the host to higher fitness levels that would otherwise be accessible  
377 only through slower microevolutionary steps (Fellous & Salvaudon, 2009). Alternatively,  
378 symbiont-induced phenotypic changes may provide new functions allowing the host to reach  
379 higher levels of fitness unlikely to be attainable through mutation. Shell colour in intertidal  
380 mussel is reasonably plastic, however, the distinctive shell whitening caused by the eroding  
381 activity of endoliths extends beyond the range of such plasticity. This pronounced phenotypic  
382 change provides mussels with a higher degree of thermal buffering that is most likely  
383 unreachable through adaptive mutation. It has been suggested that endolithic thermal  
384 buffering might be indicative of a transition towards mutualism in the endolith-mussel  
385 relationship (Gehman & Harley, 2019; Zardi et al., 2016). Indeed, most mutualisms have  
386 evolved from wholly parasitic associations and conditionally beneficial parasites are

387 intermediate stages in a transient relationship triggered by changes in the biotic/abiotic  
388 environment (Fellous & Salvaudon, 2009). The ecological advantages of endolithic infestation  
389 are likely to be increasingly important in an era of global warming and more frequent and  
390 intense heatwaves. On the other hand, recurred storm strikes are also predicted to increase  
391 potentially raising mortality rates in infested mussels as they are more weakly attached to  
392 rocky shores than non-infested mussels. Critically, the ecological advantages of mussels with  
393 corroded shells will vary spatially and temporally. Our results suggest that these benefits will  
394 potentially peak in summer and at lower latitudes when and where intense solar radiation  
395 maximises relative differences in body temperature between corroded and uncorroded  
396 mussels.

397 In order to standardise our experimental design, all robomussels used were built using  
398 *M. galloprovincialis* shells sampled from a single location in southern Portugal. In reality, our  
399 study sites supported different mussel species, including *M. galloprovincialis*/*M. edulis* hybrids  
400 in the UK and northern France (Bierne et al., 2003), raising the possibility that endolithic  
401 communities and the cooling effect observed in *M. galloprovincialis* robomussels may not  
402 apply to other species. Recent evidence indicates that endolithic community composition and  
403 the thermal benefits they confer are similar among hosts. *Perna perna*, with an aragonite shell  
404 and *M. galloprovincialis*, with aragonite and calcite shell layers, co-exist in South Africa.  
405 Despite differences in shell and periostracum structure (Bers et al., 2010), severely infested  
406 mussels of the two species support the same endolith species (Ndhlovu et al., 2020). Most  
407 importantly, both mussels exhibit the same degree of thermal buffering by endoliths under a  
408 variety of environmental conditions (Zardi et al., 2016). Together these findings support the  
409 abundant literature highlighting the generalist, nonspecific, nature of endolithic corrosion (e.g.,  
410 Golubic et al., 2005) and strongly suggest that thermal stress mitigation by symbiotic endolithic  
411 microbes does not apply to *M. galloprovincialis* only.



412 Mussel mass mortalities have repeatedly been reported globally and are often attributed to  
413 heatwaves (Harley, 2008; Petes et al., 2007; Suchanek, 1985; Tsuchiya, 1983). During the heatwave on  
414 the northern French coastline in August 2018, large numbers of empty mussel shells were washed  
415 ashore (Seuront et al., 2019). Interestingly, a close examination to over 1200 randomly shells collected  
416 following this mass mortality event show that the vast majority of them (96 to 100%) had no sign of  
417 infestation (Seuront, unpublished data, see Supplementary Material Figure S4). Although such  
418 observations cannot quantify or confirm the protective roles of endoliths, they complement previous  
419 field manipulative experiments in different regions showing that, during heat waves, the moderation  
420 of solar heating by endoliths results in significantly lower mortality rates (Gehman & Harley, 2019;  
421 Zardi et al., 2016). Interestingly, large-scale sampling covering a wide latitudinal range (ca. 28-37°N)  
422 along the coasts of Portugal and Morocco revealed a strong gradient of increasing endolithic  
423 infestation of *M. galloprovincialis* towards lower latitudes, presumably due to the enhancement of  
424 endolith photosynthetic activity through greater light availability and decreased cloud cover towards  
425 the equator (Lourenço et al., 2017). Importantly, *M. galloprovincialis* is the only *Mytilus* spp. along this  
426 coast, eliminating potential confounding effects between endolith frequency and host identity.  
427 Likewise, higher levels of shell corrosion at lower latitudes is unlikely due to latitudinal or geographic  
428 changes in endolithic species. Endolithic community composition does not differ significantly between  
429 *M. galloprovincialis* from native (Portugal) and invasive (South Africa) regions nor from *P. perna* shells  
430 from different bioregion along 1000s km of the South African coast (Marquet et al., 2013; Ndhlovu et  
431 al., 2019). Most importantly, our results indicate that endolithic corrosion is higher at lower  
432 latitudes where its beneficial effects are enhanced and most beneficial to the host. Will climate-  
433 associated thermal stress push the endolith-mussel relationship towards a long-lasting  
434 mutually beneficial association? This seems possible as heatwaves are increasing in intensity,  
435 frequency and duration and these trends are expected to strengthen under future climatic  
436 changes (Perkins-Kirkpatrick et al., 2020; Smale et al., 2019). Further work is required to

437 evaluate if the cooling effect of endoliths has a significant impact on mussel fitness and if the  
438 average fitness of corroded hosts, across all possible environments, is higher than that of  
439 uncorroded individuals. Such an approach will also be key to testing the validity of near-future  
440 conditions under which mussels shift their ecological niche to one whereby endoliths are more  
441 often advantageous or might even evolve endolith dependence, losing the ability to live without  
442 their symbionts.

443

444         Although hosts and symbionts have coupled life cycles, they can respond differently to  
445 environmental changes. Thus, the response of host–symbiont interactions to climate warming  
446 may largely depend on the performance of each interactor and the influence of the symbiont  
447 on host performance (Gehman et al., 2018; Lafferty et al., 2003). In this context, mussel  
448 survival may increasingly benefit from the thermal buffering provided by endolithic shell  
449 erosion, which is predicted to increase as a result of ongoing ocean acidification and warming  
450 rates (Reyes-Nivia et al., 2013; Tribollet et al., 2009). A further complication lies in the fact that  
451 the endoliths infesting mussel shells comprise a community, the composition of which alters  
452 in time and space (Ndhlovu et al., 2019; Pittera et al., 2014). Nevertheless, the generalist  
453 nature of endoliths and their ubiquitous erosion of marine calcifying organisms  
454 already stretched to the limits of their thermal tolerances strongly suggest that they will have  
455 a key influence on the ability of many intertidal ecosystems to maintain their ecological  
456 functions.

457

## 458 **ACKNOWLEDGEMENTS**

459 This work has also been financially supported by a Pierre Hubert Curien PESSOA Fellowship,  
460 projects UIDB/04326/2020 from the Fundação para a Ciência e Tecnologia (FCT-MEC,  
461 Portugal) and Grant number 64801 from the National Research Foundation of South Africa,  
462 and a South African Research Chairs Initiative (SARChI) of the Department of Science and

463 Technology and the National Foundation and a scholarship from the South African National  
464 Research Foundation (NRF). This work is a contribution to the CPER research project  
465 CLIMIBIO. The authors thank the French Ministère de l'Enseignement Supérieur et de la  
466 Recherche, the Hauts de France Region and the European Funds for Regional Economical  
467 Development for their financial support for this project.

468

## 469 REFERENCES

470 Akaike, H. (1974). A new look at the statistical model identification. *IEEE Transactions on*  
471 *Automatic Control*, 19, 716-723.

472 Altizer, S., Ostfeld, R. S., Johnson, P. T., Kutz, S., & Harvell, C. D. (2013). Climate change  
473 and infectious diseases: from evidence to a predictive framework. *Science*,  
474 341(6145), 514-519.

475 Arbuckle, K., & Speed, M. P. (2015). Antipredator defenses predict diversification rates.  
476 *Proceedings of the National Academy of Sciences*, 112(44), 13597-13602.

477 Arias-Ortiz, A., Serrano, O., Masqué, P., Lavery, P. S., Mueller, U., Kendrick, G. A., . . .  
478 Duarte, C. M. (2018). A marine heatwave drives massive losses from the world's  
479 largest seagrass carbon stocks. *Nature Climate Change*, 8(4), 338-344.  
480 doi:10.1038/s41558-018-0096-y

481 Bates, D., Mächler, M., Bolker, B., & Walker, S. (2015). Fitting linear mixed-effects models  
482 using lme4. *Journal of Statistical Software*, 67(1), 1-48. doi:10.18637/jss.v067.i01

483 Bers, A., Díaz, E., Da Gama, B., Vieira-Silva, F., Dobretsov 3, S., Valdivia 4, N., . . . Sudgen  
484 6, H. (2010). Relevance of mytilid shell microtopographies for fouling defence—a  
485 global comparison. *Biofouling*, 26(3), 367-377.

486 Bierne, N., Borsa, P., Daguin, C., Jollivet, D., Viard, F., Bonhomme, F., & David, P. (2003).  
487 Introgression patterns in the mosaic hybrid zone between *Mytilus edulis* and *M.*  
488 *galloprovincialis*. *Molecular Ecology*, 12(2), 447-461.

489 Brumin, M., Kontsedalov, S., & Ghanim, M. (2011). Rickettsia influences thermotolerance in  
490 the whitefly Bemisia tabaci B biotype. *Insect Science*, 18(1), 57-66.

- 491 Burnette, M. F., & Ashley-Ross, M. A. (2015). One shot, one kill: the forces delivered by  
492 archer fish shots to distant targets. *Zoology*, 118(5), 302-311.
- 493 Burnham, K. P., & Anderson, D. R. (2002). *Model selection and multimodel inference: A*  
494 *practical information-theoretic approach*. New York: Springer-Verlag.
- 495 Chomicki, G., Kiers, E. T., & Renner, S. S. (2020). The evolution of mutualistic dependence.  
496 *Annual Review of Ecology, Evolution, and Systematics*, 51.
- 497 Costanza, R., d'Arge, R., De Groot, R., Farber, S., Grasso, M., Hannon, B., . . . Paruelo, J.  
498 (1997). The value of the world's ecosystem services and natural capital. *nature*,  
499 387(6630), 253-260.
- 500 FAO. (2020). *GLOBEFISH Highlights - A quarterly update on world seafood markets. with*  
501 *Jan. – Jun. 2019 Statistics – A quarterly update on world seafood markets*. Retrieved  
502 from
- 503 Feldhaar, H. (2011). Bacterial symbionts as mediators of ecologically important traits of  
504 insect hosts. *Ecological Entomology*, 36(5), 533-543.
- 505 Fellous, S., & Salvaudon, L. (2009). How can your parasites become your allies? *Trends in*  
506 *Parasitology*, 25(2), 62-66. doi:10.1016/j.pt.2008.11.010
- 507 Firth, L. B. (2017). Factors affecting the prevalence of the trematode parasite *Echinostephilla*  
508 *patellae* (Lebour, 1911) in the limpet *Patella vulgata* (L.). *Journal of Experimental*  
509 *Marine Biology and Ecology*, v. 492, pp. 99-104-2017 v.2492.  
510 doi:10.1016/j.jembe.2017.01.026
- 511 Fischer, E. M., & Schär, C. (2010). Consistent geographical patterns of changes in high-  
512 impact European heatwaves. *Nature Geoscience*, 3(6), 398-403.  
513 doi:10.1038/ngeo866
- 514 Fitzhenry, T., Halpin, P. M., & Helmuth, B. (2004). Testing the effects of wave exposure, site,  
515 and behavior on intertidal mussel body temperatures: applications and limits of  
516 temperature logger design. *Marine Biology*, 145(2), 339-349. doi:10.1007/s00227-  
517 004-1318-6
- 518 Futuyma, D. J., & Moreno, G. (1988). The evolution of ecological specialization. *Annual*  
519 *Review of Ecology and Systematics*, 29, 207-233

- 520 Galis, F. (2001). Key innovations and radiations. *The character concept in evolutionary*  
521 *biology*.
- 522 Garcia-Pichel, F., Ramírez-Reinat, E., & Gao, Q. (2010). Microbial excavation of solid  
523 carbonates powered by P-type ATPase-mediated transcellular Ca<sup>2+</sup> transport.  
524 *Proceedings of the National Academy of Sciences*, 107(50), 21749-21754.  
525 doi:10.1073/pnas.1011884108
- 526 Gehman, A.-L. M., Hall, R. J., & Byers, J. E. (2018). Host and parasite thermal ecology  
527 jointly determine the effect of climate warming on epidemic dynamics. *Proceedings of*  
528 *the National Academy of Sciences*, 115(4), 744-749.
- 529 Gehman, A.-L. M., & Harley, C. D. G. (2019). Symbiotic endolithic microbes alter host  
530 morphology and reduce host vulnerability to high environmental temperatures.  
531 *Ecosphere*, 10(4), e02683. doi:<https://doi.org/10.1002/ecs2.2683>
- 532 Gilman, S. E., Harley, C. D. G., Strickland, D. C., Vanderstraeten, O., O'Donnell, M. J., &  
533 Helmuth, B. (2006). Evaluation of effective shore level as a method of characterizing  
534 intertidal wave exposure regimes. *Limnol. Oceanogr. Methods*, 4, 448–445.  
535 doi:<https://doi.org/10.4319/lom.2006.4.448>
- 536 Golubic, S., Radtke, G., & Le Campion-Alsumard, T. (2005). Endolithic fungi in marine  
537 ecosystems. *Trends in Microbiology*, 13(5), 229-235.
- 538 Halpern, B. S., Walbridge, S., Selkoe, K. A., Kappel, C. V., Micheli, F., D'Agrosa, C., . . .  
539 Watson, R. (2008). A global map of human impact on marine ecosystems. *Science*,  
540 319(5865), 948-952. doi:10.1126/science.1149345
- 541 Harley, C. D. (2008). Tidal dynamics, topographic orientation, and temperature-mediated  
542 mass mortalities on rocky shores. *Marine Ecology Progress Series*, 371, 37-46.
- 543 Harley, C. D. G. (2011). Climate change, keystone predation, and biodiversity loss. *Science*,  
544 334(6059), 1124-1127. doi:10.1126/science.1210199
- 545 Harley, C. D. G., & Helmuth, B. S. T. (2003). Local- and regional-scale effects of wave  
546 exposure, thermal stress, and absolute versus effective shore level on patterns of  
547 intertidal zonation. *Limnol. Oceanogr.*, 48(4), 1498–1508.  
548 doi:<https://doi.org/10.4319/lo.2003.48.4.1498>

- 549 Harvell, D., Altizer, S., Cattadori, I. M., Harrington, L., & Weil, E. (2009). Climate change and  
550 wildlife diseases: When does the host matter the most? *Ecology*, 90(4), 912-920.  
551 doi:10.1890/08-0616.1
- 552 Helmuth, B. (2002). How do we measure the environment? Linking intertidal thermal  
553 physiology and ecology through biophysics. *Integrative and comparative biology*,  
554 42(4), 837-845.
- 555 Helmuth, B., Broitman, B. R., Yamane, L., Gilman, S. E., Mach, K., Mislán, K. A. S., &  
556 Denny, M. W. (2010). Organismal climatology: analyzing environmental variability at  
557 scales relevant to physiological stress. *Journal of Experimental Biology*, 213(6), 995-  
558 1003. doi:10.1242/jeb.038463
- 559 Helmuth, B., Choi, F., Matzelle, A., Torossian, J. L., Morello, S. L., Mislán, K. A. S., . . .  
560 Zardi, G. (2016). Long-term, high frequency in situ measurements of intertidal mussel  
561 bed temperatures using biomimetic sensors. *Scientific Data*, 3, 160087.  
562 doi:10.1038/sdata.2016.87
- 563 Helmuth, B. S. T. (1998). Intertidal mussel microclimates: predicting the body temperature of  
564 a sessile invertebrate. *Ecological Monographs*, 68(1), 51-74. doi:doi:10.1890/0012-  
565 9615(1998)068[0051:IMMPTB]2.0.CO;2
- 566 Hobday, A. J., Oliver, E. C. J., Gupta, A. S., Benthuyssen, J. A., Burrows, M. T., Donat, M. G.,  
567 . . . Smale, D. A. (2018). Categorizing and naming marine heatwaves.  
568 *Oceanography*, 31(2), 162–173. doi:10.5670/oceanog.2018.205
- 569 Holbrook, N. J., Gupta, A. S., Oliver, E. C., Hobday, A. J., Benthuyssen, J. A., Scannell, H. A.,  
570 . . . Wernberg, T. (2020). Keeping pace with marine heatwaves. *Nature Reviews*  
571 *Earth & Environment*, 1-12.
- 572 Hughes, T. P., Kerry, J. T., Álvarez-Noriega, M., Álvarez-Romero, J. G., Anderson, K. D.,  
573 Baird, A. H., . . . Berkelmans, R. (2017). Global warming and recurrent mass  
574 bleaching of corals. *nature*, 543(7645), 373-377.
- 575 Hunter, J. P. (1998). Key innovations and the ecology of macroevolution. *Trends in ecology*  
576 *& evolution*, 13(1), 31-36.

- 577 Janson, E. M., Stireman III, J. O., Singer, M. S., & Abbot, P. (2008). Phytophagous insect–  
578 microbe mutualisms and adaptive evolutionary diversification. *Evolution: International*  
579 *Journal of Organic Evolution*, 62(5), 997-1012.
- 580 Kaehler, S., & McQuaid, C. D. (1999). Lethal and sub-lethal effects of phototrophic endoliths  
581 attacking the shell of the intertidal mussel *Perna perna*. *Marine Biology*, 135(3), 497-  
582 503. doi:10.1007/s002270050650
- 583 Lafferty, K. D., & Holt, R. D. (2003). How should environmental stress affect the population  
584 dynamics of disease? *Ecology Letters*, 6(7), 654-664.
- 585 Li, L., Hollowed, A. B., Cokelet, E. D., Barbeaux, S. J., Bond, N. A., Keller, A. A., . . .  
586 Stabeno, P. J. (2019). Subregional differences in groundfish distributional responses  
587 to anomalous ocean bottom temperatures in the northeast Pacific. *Global change*  
588 *biology*, 25(8), 2560-2575.
- 589 Lourenço, C. R., Nicastro, K. R., McQuaid, C. D., Sabour, B., & Zardi, G. I. (2017).  
590 Latitudinal incidence of phototrophic shell-degrading endoliths and their effects on  
591 mussel bed microclimates. *Marine Biology*, 164(6), 129.
- 592 Macnab, V., & Barber, I. (2012). Some (worms) like it hot: fish parasites grow faster in  
593 warmer water, and alter host thermal preferences. *Global change biology*, 18(5),  
594 1540-1548.
- 595 Macreadie, P. I., Anton, A., Raven, J. A., Beaumont, N., Connolly, R. M., Friess, D. A., . . .  
596 Duarte, C. M. (2019). The future of Blue Carbon science. *Nature communications*,  
597 10(1), 3998. doi:10.1038/s41467-019-11693-w
- 598 Maga, E. A. (2020). UC Davis Transgenic Animal Research Conference XII (TARC XII).  
599 *Transgenic Research*, 29(4), 461-465. doi:10.1007/s11248-020-00206-x
- 600 Marquet, N., Nicastro, K. R., Gektidis, M., McQuaid, C. D., Pearson, G. A., Serrão, E. A., &  
601 Zardi, G. I. (2013). Comparison of phototrophic shell-degrading endoliths in invasive  
602 and native populations of the intertidal mussel *Mytilus galloprovincialis*. *Biological*  
603 *Invasions*, 15(6), 1253-1272. doi:10.1007/s10530-012-0363-1
- 604 Marshall, D. J., McQuaid, C. D., & Williams, G. A. (2010). Non-climatic thermal adaptation:  
605 implications for species' responses to climate warming. *Biology Letters*, 6(5), 669-  
606 673. doi:10.1098/rsbl.2010.0233

- 607 Met Office. (2019a). MIDAS Open: UK hourly rainfall data, v201908. *Centre for*  
608 *Environmental Data Analysis*, 30 October 2019.  
609 doi:<https://doi.org/10.5285/a58b9c8a724e4ec795a40a74455462b7>
- 610 Met Office. (2019b). MIDAS Open: UK hourly solar radiation data, v201908. *Centre for*  
611 *Environmental Data Analysis*, 30 October 2019.  
612 doi:<https://doi.org/10.5285/d6bbe115245042dc93ee68caa253d60b>
- 613 Met Office. (2019c). MIDAS Open: UK hourly weather observation data, v201908. *Centre for*  
614 *Environmental Data Analysis*, 30 October 2019.  
615 doi:<https://doi.org/10.5285/6c441aea187b44819b9e929e575b0d7e>
- 616 Miller, A. H. (1949). Some ecologic and morphologic considerations in the evolution of higher  
617 taxonomic categories. *Ornithologie als biologische Wissenschaft*, 28, 84-88.
- 618 Miller, L. P., & Dowd, W. W. (2017). Multimodal in situ datalogging quantifies inter-individual  
619 variation in thermal experience and persistent origin effects on gaping behavior  
620 among intertidal mussels (*Mytilus californianus*). *Journal of Experimental Biology*,  
621 220(22), 4305-4319.
- 622 Moyen, N. E., Somero, G. N., & Denny, M. W. (2019). Impact of heating rate on cardiac  
623 thermal tolerance in the California mussel, *Mytilus californianus*. *Journal of*  
624 *Experimental Biology*, 222(17), jeb203166.
- 625 Ndhlovu, A., McQuaid, C. D., & Monaco, C. J. (2021). Ectoparasites reduce scope for growth  
626 in a rocky-shore mussel (*Perna perna*) by raising maintenance costs. *Science of The*  
627 *Total Environment*, 753, 142020. doi:<https://doi.org/10.1016/j.scitotenv.2020.142020>
- 628 Ndhlovu, A., McQuaid, C. D., Nicastro, K., Marquet, N., Gektidis, M., Monaco, C. J., & Zardi,  
629 G. (2019). Biogeographical Patterns of Endolithic Infestation in an Invasive and an  
630 Indigenous Intertidal Marine Ecosystem Engineer. *Diversity*, 11(5), 75.
- 631 Ndhlovu, A., McQuaid, C. D., Nicastro, K. R., & Zardi, G. I. (2020). Community succession in  
632 phototrophic shell-degrading endoliths attacking intertidal mussels. *Journal of*  
633 *Molluscan Studies*. doi:10.1093/mollus/eyaa036
- 634 Nicastro, K. R., McQuaid, C. D., Dievart, A., & Zardi, G. I. (2020). Intraspecific diversity in an  
635 ecological engineer functionally trumps interspecific diversity in shaping community



- 636 structure. *Science of The Total Environment*, 743, 140723.  
637 doi:<https://doi.org/10.1016/j.scitotenv.2020.140723>
- 638 Nicastro, K. R., McQuaid, C. D., & Zardi, G. I. (2018). Between a rock and a hard place:  
639 combined effect of trampling and phototrophic shell-degrading endoliths in marine  
640 intertidal mussels. *Marine Biodiversity*, 1-6.
- 641 Nicastro, K. R., Zardi, G. I., McQuaid, C. D., Pearson, G. A., & Serrão, E. A. (2012). Love  
642 Thy Neighbour: Group Properties of Gaping Behaviour in Mussel Aggregations.  
643 *PLoS One*, 7(10), e47382. doi:<https://doi.org/10.1371/journal.pone.0047382>
- 644 Nowakowski, A. J., Whitfield, S. M., Eskew, E. A., Thompson, M. E., Rose, J. P., Caraballo,  
645 B. L., . . . Todd, B. D. (2016). Infection risk decreases with increasing mismatch in  
646 host and pathogen environmental tolerances. *Ecology Letters*, 19(9), 1051-1061.
- 647 Oliver, E. C., Donat, M. G., Burrows, M. T., Moore, P. J., Smale, D. A., Alexander, L. V., . . .  
648 Hobday, A. J. (2018). Longer and more frequent marine heatwaves over the past  
649 century. *Nature communications*, 9(1), 1-12.
- 650 Perkins-Kirkpatrick, S. E., & Lewis, S. C. (2020). Increasing trends in regional heatwaves.  
651 *Nature communications*, 11(1), 3357. doi:10.1038/s41467-020-16970-7
- 652 Petes, L. E., Menge, B. A., & Murphy, G. D. (2007). Environmental stress decreases  
653 survival, growth, and reproduction in New Zealand mussels. *Journal of Experimental*  
654 *Marine Biology and Ecology*, 351(1-2), 83-91.
- 655 Pinheiro, J., Bates, D., DebRoy, S., Sarkar, D., & R Core Team. (2020). nlme: Linear and  
656 Nonlinear Mixed Effects Models. <https://CRAN.R-project.org/package=nlme>: R  
657 package version 3.1-151.
- 658 Pittera, J., Humily, F., Thorel, M., Grulois, D., Garczarek, L., & Six, C. (2014). Connecting  
659 thermal physiology and latitudinal niche partitioning in marine *Synechococcus*. *The*  
660 *ISME journal*, 8(6), 1221-1236.
- 661 Porter, W. P., & Gates, D. M. (1969). Thermodynamic Equilibria of Animals with  
662 Environment. *Ecol. Monogr.*, 39(3), 227-244. doi:<https://doi.org/10.2307/1948545>
- 663 Rabosky, D. L. (2014). Automatic detection of key innovations, rate shifts, and diversity-  
664 dependence on phylogenetic trees. *PLoS One*, 9(2), e89543.

- 665 Raffaelli, D., & Hawkins, S. J. (2012). *Intertidal ecology*. Springer Science & Business Media.
- 666 Rahmstorf, S., & Coumou, D. (2011). Increase of extreme events in a warming world.  
667 *Proceedings of the National Academy of Sciences*, 108(44), 17905.  
668 doi:10.1073/pnas.1101766108
- 669 Reyes-Nivia, C., Diaz-Pulido, G., Kline, D., Guldberg, O. H., & Dove, S. (2013). Ocean  
670 acidification and warming scenarios increase microbioerosion of coral skeletons.  
671 *Global change biology*, 19(6), 1919-1929.
- 672 Santos, J. C., Coloma, L. A., & Cannatella, D. C. (2003). Multiple, recurring origins of  
673 aposematism and diet specialization in poison frogs. *Proceedings of the National*  
674 *Academy of Sciences*, 100(22), 12792-12797.
- 675 Sauer, E. L., Fuller, R. C., Richards-Zawacki, C. L., Sonn, J., Sperry, J. H., & Rohr, J. R.  
676 (2018). Variation in individual temperature preferences, not behavioural fever, affects  
677 susceptibility to chytridiomycosis in amphibians. *Proceedings of the Royal Society B:*  
678 *Biological Sciences*, 285(1885), 20181111.
- 679 Schuster, S., Wöhl, S., Griebisch, M., & Klostermeier, I. (2006). Animal cognition: how archer  
680 fish learn to down rapidly moving targets. *Current Biology*, 16(4), 378-383.
- 681 Seabra, R., Wetthey, D. S., Santos, A. M., & Lima, F. P. (2015). Understanding complex  
682 biogeographic responses to climate change. *Scientific Reports*, 5(1), 1-6.
- 683 Seuront, L., Nicastro, K. R., Zardi, G. I., & Goberville, E. (2019). Decreased thermal  
684 tolerance under recurrent heat stress conditions explains summer mass mortality of  
685 the blue mussel *Mytilus edulis*. *Scientific Reports*, 9(1), 17498. doi:10.1038/s41598-  
686 019-53580-w
- 687 Smale, D. A., Wernberg, T., Oliver, E. C. J., Thomsen, M., Harvey, B. P., Straub, S. C., . . .  
688 Moore, P. J. (2019). Marine heatwaves threaten global biodiversity and the provision  
689 of ecosystem services. *Nature Climate Change*, 9(4), 306-312. doi:10.1038/s41558-  
690 019-0412-1
- 691 Stillman, J. H. (2019). Heat Waves, the New Normal: Summertime Temperature Extremes  
692 Will Impact Animals, Ecosystems, and Human Communities. *Physiology*, 34(2), 86-  
693 100. doi:10.1152/physiol.00040.2018

- 694 Suchanek, T. (1985). Mussels and their role in structuring rocky shore communities. *The*  
695 *Ecology of Rocky Coastes*, 70-96.
- 696 Summers, K. (2003). Convergent evolution of bright coloration and toxicity in frogs.  
697 *Proceedings of the National Academy of Sciences*, 100(22), 12533-12534.
- 698 Tribollet, A., Godinot, C., Atkinson, M., & Langdon, C. (2009). Effects of elevated pCO<sub>2</sub> on  
699 dissolution of coral carbonates by microbial euendoliths. *Global Biogeochemical*  
700 *Cycles*, 23(3).
- 701 Tsuchiya, M. (1983). Mass mortality in a population of the mussel *Mytilus edulis* L. caused  
702 by high temperature on rocky shores. *Journal of Experimental Marine Biology*  
703 *Ecology*, 66, 101-111.
- 704 Wernberg, T., Smale, D. A., Tuya, F., Thomsen, M. S., Langlois, T. J., de Bettignies, T., . . .  
705 Rousseaux, C. S. (2013). An extreme climatic event alters marine ecosystem  
706 structure in a global biodiversity hotspot. *Nature Clim. Change*, 3(1), 78-82.  
707 doi:[http://www.nature.com/nclimate/journal/v3/n1/abs/nclimate1627.html#supplement](http://www.nature.com/nclimate/journal/v3/n1/abs/nclimate1627.html#supplementary-information)  
708 [ary-information](http://www.nature.com/nclimate/journal/v3/n1/abs/nclimate1627.html#supplementary-information)
- 709 Zardi, G., Nicastro, K., McQuaid, C., Ng, T., Lathlean, J., & Seuront, L. (2016). Enemies with  
710 benefits: parasitic endoliths protect mussels against heat stress. *Scientific Reports*, 6,  
711 31413.
- 712 Zardi, G. I., Nicastro, K. R., McQuaid, C. D., & Gektidis, M. (2009). Effects of endolithic  
713 parasitism on invasive and indigenous mussels in a variable physical environment.  
714 *PLoS One*, 4(8), e6560.
- 715
- 716

717 **TABLES**

718 **Table 1. Main drivers of the maximum difference in body temperature between non-**  
 719 **infested and infested mussels.** Results are shown for all best candidate models ( $\Delta AICc <$   
 720  $2$ ) as compared to the null model, along with associated Akaike weights (relative support of  
 721 each model). The selected model (least number of parameters) is indicated in bold.

Meteorological parameters (estimated coefficients $\pm$ SE)	AICc	$\Delta AICc$	Akaike weights
Intercept(0.51 $\pm$ 0.35) + AT(-0.03 $\pm$ 0.02) + SR(0.05 $\pm$ 0.005) + WS(-0.04 $\pm$ 0.01) + Rdm(SD=0.24)	1845.13	0	0.28
<b>Intercept(0.09<math>\pm</math>0.16) + SR(0.05<math>\pm</math>0.005) + WS(-0.04<math>\pm</math>0.01) + Rdm(SD=0.24)</b>	<b>1845.34</b>	<b>0.21</b>	<b>0.25</b>
Intercept(0.66 $\pm$ 0.36) + SR(0.04 $\pm$ 0.007) + RH(-0.006 $\pm$ 0.004) + WS(-0.04 $\pm$ 0.01) + Rdm(SD=0.24)	1845.88	0.75	0.19
Intercept(0.94 $\pm$ 0.48) + AT(-0.02 $\pm$ 0.02) + SR(0.05 $\pm$ 0.007) + RH(-0.005 $\pm$ 0.004) + WS(-0.04 $\pm$ 0.01) + Rdm(SD=0.25)	1846.14	1.02	0.17
Intercept(0.50 $\pm$ 0.35) + AT(-0.03 $\pm$ 0.02) + SR(0.05 $\pm$ 0.005) + PR(0.002 $\pm$ 0.005) + WS(-0.04 $\pm$ 0.01) + Rdm(SD=0.24)	1847.01	1.88	0.11
null	1969.24	124.12	0

722 Abbreviations: Solar Radiation (SR), Relative Humidity (RH), Wind Speed (WS), Air  
 723 Temperature (AT) and Precipitation (PR), Random factor (Rdm; robomussel identity nested  
 724 within locations).

725

726 **Table 2. Meteorological conditions during heatwaves identified in 2018 at Wimereux,**  
 727 **France.** Heat waves were identified based on air temperature during summer 2018, and were  
 728 classified from moderate to extreme: “These events were classified as moderate (78.1%) to  
 729 strong (21.9%) in June, moderate (67.8%), strong (23.1%), severe (7.0%) and extreme (2.0%)  
 730 in July, and moderate (63.0%), strong (30.9%) and severe (6.2%) in August.” (from Seuront  
 731 et al. 2019). Maximum temperature differences between non-infested and infested mussels

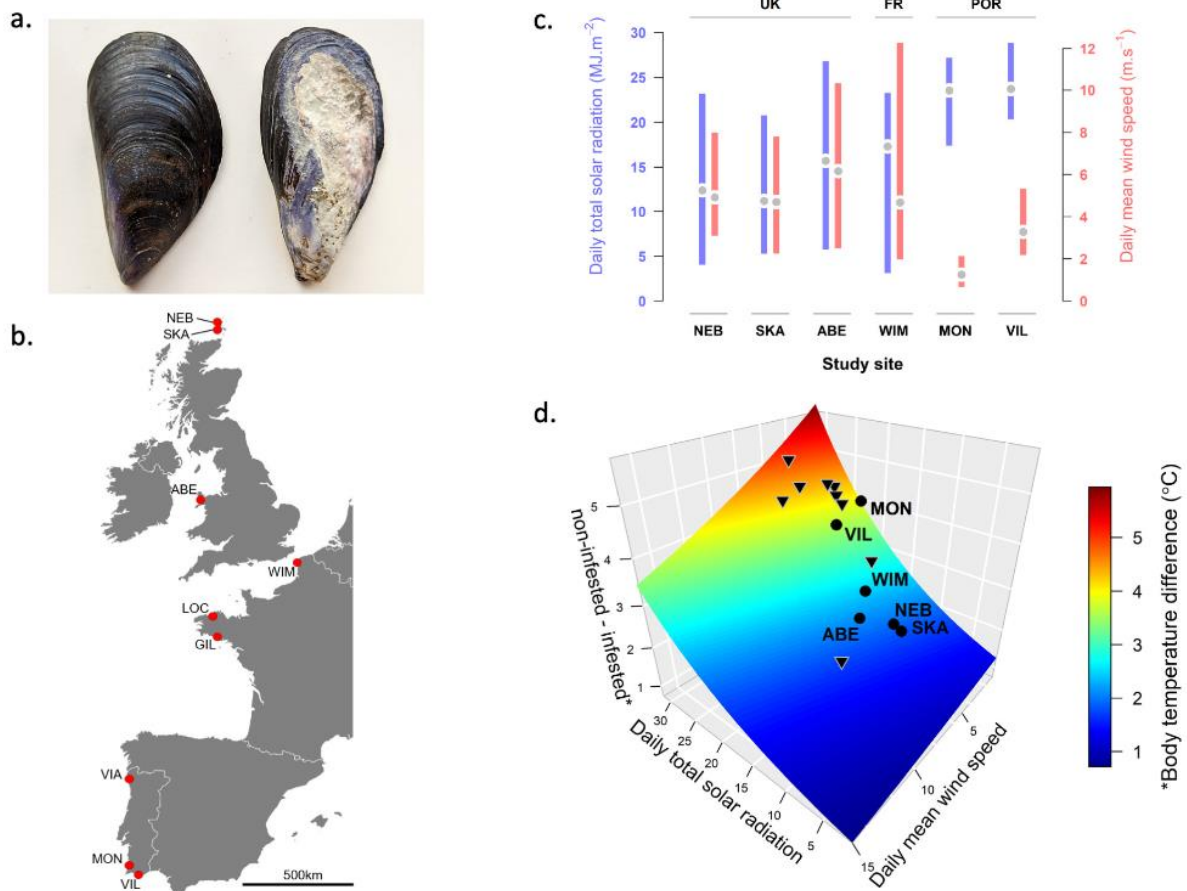
732 were predicted based on wind speed and solar radiation using the model selected in the  
 733 present study.

Date (in 2018)	Mean daily wind speed (m.s <sup>-1</sup> )	Mean daily total solar radiation (MJ.m <sup>-2</sup> )	Predicted max. temperature differences (°C) (95% confidence intervals)
June 28 to 30	4.54	28.160	4.26 (1.15)
July 05 to 07	2.48	26.006	4.14 (1.12)
July 23 to 25	2.61	24.433	3.80 (1.11)
August 01 to 08	2.67	25.350	3.97 (1.11)
June 23	2.81	26.610	4.21 (1.13)
June 26	4.41	30.270	4.77 (1.17)
July 13	3.12	18.510	2.75 (1.08)
July 17	5.95	28.350	4.06 (1.17)
August 10	8.95	13.340	1.67 (1.12)

734

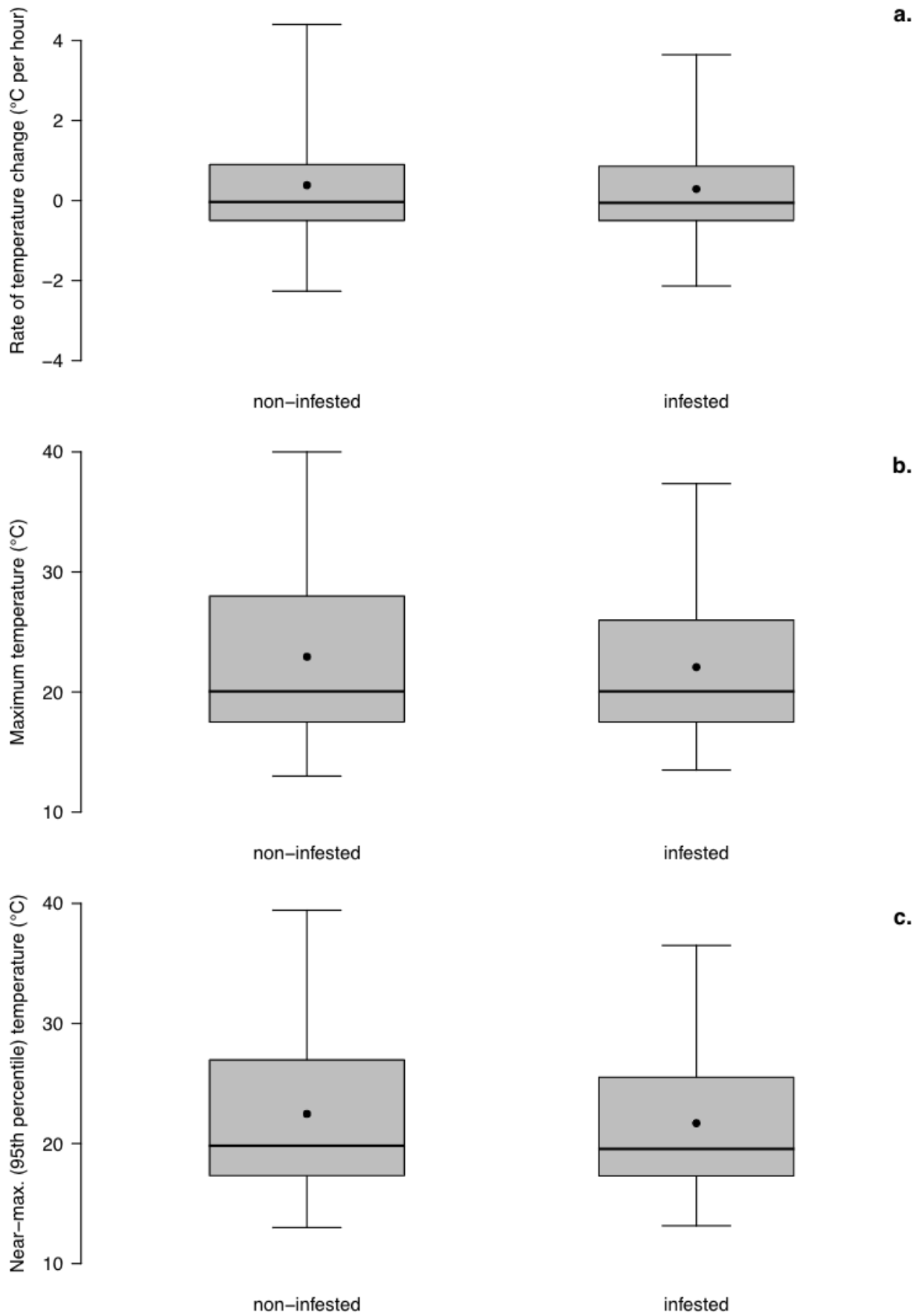
735

736 **FIGURE LEGENDS**



737

738 **Fig. 1.** (a) Example of non-infested and infested mussels. (b) Study sites where mussels were  
739 deployed. (c) Daily total (global) solar radiation (blue) and mean wind speed (red) during  
740 emergence at (from north (left) to south (right)) Nebo Geo (NEB), Bay of Skail (SKA) and  
741 Aberffraw (ABE), United Kingdom (UK), Wimereux (WIM), France (FR) and, Monte Clerigo  
742 (MON) and Vilamoura (VIL), Portugal (POR). Coloured bars indicate 2.5<sup>th</sup> and 97.5<sup>th</sup>  
743 percentiles and grey points are the median values. (d) Prediction surface of maximum  
744 temperature differences in body temperature between non-infested and infested mussels (see  
745 Supplementary Fig. S2 for a 2D representation with confidence intervals): The daily maximum  
746 difference increases with increasing solar radiation and decreasing wind speed (units are  
747 displayed in panel c). Black points indicate the mean expected difference for each site using  
748 data averaged over the study period and triangles indicate the mean expected difference  
749 during nine heatwaves identified at Wimereux during summer 2018 (confidence intervals are  
750 between +/-1.08°C and +/-1.15°C for predictions during heatwaves; see Table 2).



752 **Fig. 2. Comparison of the temperature response between non-infested and infested**  
753 **mussels.** (a) Average rate of change in body temperatures and (b) maximum or (c) near-  
754 maximum (95<sup>th</sup> percentile) temperatures (per tidal cycles) during emergence. Means (black  
755 dots), medians (central bars), 2.5<sup>th</sup> and 97.5<sup>th</sup> percentiles (respectively, lower and upper bars),  
756 and 25<sup>th</sup> and 75<sup>th</sup> percentiles (grey boxes) are shown.

757

758